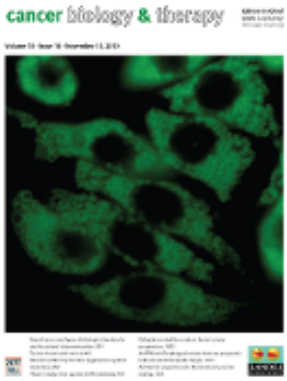

Cancer Biology & Therapy
Publication details, including instructions for authors and subscription information:
http://www.tandfonline.com/loi/kcbt20

Rose Bengal Acetate photodynamic therapy-induced autophagy

Luciana Dini, Valentina Inguscio, Bernardetta Tenuzzo & Elisa Panzarini

Published online: 15 Nov 2010.

To cite this article: Luciana Dini, Valentina Inguscio, Bernardetta Tenuzzo & Elisa Panzarini (2010) Rose Bengal Acetate photodynamic therapy-induced autophagy , Cancer Biology & Therapy, 10:10, 1048-1055, DOI: 10.4161/cbt.10.10.13371

To link to this article: http://dx.doi.org/10.4161/cbt.10.10.13371

Cancer Biology & Therapy 10:10, 1048-1055; November 15, 2010; © 2010 Landes Bioscience

Rose bengal acetate photodynamic therapy-induced autophagy

Luciana Dini,* Valentina Inguscio, Bernardetta Tenuzzo and Elisa Panzarini

Dept. of Biological and Environmental Science and Technology (Di.S.Te.B.A.); University of Salento; Lecce Italy

Key words: rose bengal acetate, autophagy, endoplasmic reticulum, photodynamic therapy, anticancer therapy

Photodynamic therapy (PDT), an anticancer therapy requiring the exposure of cells or tissue to a photosensitizing drug followed by irradiation with visible light of the appropriate wavelength, induces cell death by the efficient induction of apoptotic as well as non-apoptotic mechanisms, such as necrosis and autophagy, or a combination of all three mechanisms. However, the exact role of autophagy in photodynamic therapy is still a matter of debate. To understand the role of autophagy in PDT, we investigated the induction of autophagy in HeLa cells photosensitized with Rose Bengal Acetate (RBAc). After incubation with Rose Bengal Acetate (10-5 M), HeLa cells were irradiated for 90 seconds (green LED DPL 305, emitting at 530 +15 nm to obtain 1.6 J/cm2 as the total light dose) and allowed to recover for 72 h. Induction of autophagy and apoptosis were observed with peaks at 8 h and 12 h after irradiation, respectively. Autophagy was detected by biochemical (western blotting for the LC3B protein) and morphological criteria (TEM, cytochemistry). In addition, the pan-caspase inhibitor, z-VAD, was unable to completely prevent cell death. The simultaneous onset of apoptosis and autophagy following Rose Bengal Acetate PDT is of remarkable interest in light of the findings that autophagy can result in the class II presentation of antigens and thus, explain why low dose PDT can yield antitumor immune responses.

Introduction

Phodynamic therapy (PDT) involves the photosensitization of cancerous cells and tissues with photosensitizing drugs (PS) that catalyze, upon irradiation, formation of reactive oxygen species.[1] PDT is a minimally invasive therapeutic modality approved for treatment of cancer diseases and non-oncological disorders.[2] In the PDT, beside vascular shutdown and immunological response, there is a direct cell kill that is able to reduce neoplastic cell population 2–3 times.[3] Cell death in PDT has been initially believed to occur via necrosis,[4] and the important contribution of apoptosis has been described by Oleinick's group only in the 1991.[5] However, the cytotoxicity of the PDT protocols cannot be explained only in terms of apoptosis or necrosis. In Bax and Bak deficient murine embryonal fibroblasts[6,7] in which the apoptosis is blocked, or in cells lacking procaspase-3,[8] the PDT treatment gave rise to cell deaths that did not display the ultrastructural and biochemical features of apoptosis or necrosis, but showed autophagy. Induction of autophagic cell death after PDT has been reported.[9-13] In fact, the efficient induction of apoptosis as well as autophagy and non-apoptotic cell deaths (e.g., necrosis), or a combination of the three mechanisms, is dependent on the PS, the PDT dose, the intracellular localization of PS, the cell metabolic potential and the cell genotype.[14]

Autophagy is distinguished by a lysosomal-dependent digestion of the cell and by the presence of autophagic vacuoles in which cytosol and organelles are encased. Autophagy is a survival response to nutrient deprivation and other forms of cellular stress. Moreover, during the last decade, data have accumulated indicating that autophagy can also induce cell death. The autophagic cell death could derive by the metabolic and bioenergetic collapse, since autophagy is a self-limiting process.[15] Autophagy deaths are important during development.[16]

Autophagy develops in sequential steps with defined morphological and biochemical characteristics that are distinct from apoptosis and necrosis;[17] thus it is referred as the second type of programmed cell death (type II cell death).

It has been recently reported that apoptosis and autophagy (via mitochondrial apoptosis and SER damage respectively) can be simultaneously induced by PDT.[9,10,18] The concomitant engagement of both apoptosis and autophagy occurs in HeLa cells following hypericin-mediated PDT regardless of a reduction in the expression levels of anti-apoptotic Bcl2 proteins, thus suggesting that autophagy plays a key role in cell death-induced PDT.[19] Since the exact role of autophagy in apoptosis-competent cells following PDT is still a matter of debate, in this study we elucidate the occurrence of autophagy in RBAc-PDT treated HeLa cells.

Results

RBAc-PDT mediated modifications of lysosomes, mitochondria and ER. Death of HeLa cells was induced by RBAc-PDT

*Correspondence to: Luciana Dini; Email: luciana.dini@unisalento.it
Submitted: 05/05/10; Revised: 07/27/10; Accepted: 08/19/10
Previously published online: www.landesbioscience.com/journals/cbt/article/13371
DOI: 10.4161/cbt.10.10.13371

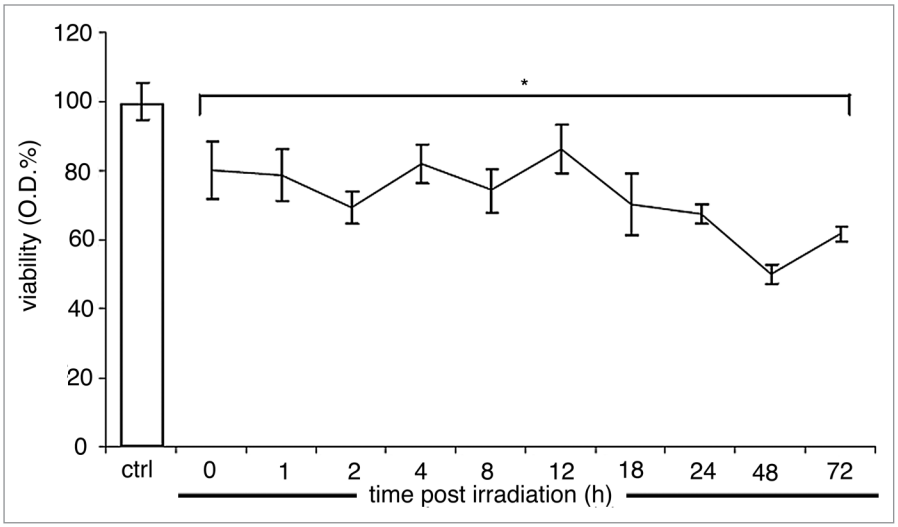

Figure 1. MTT assay performed in HeLa cells after treatment with RBAc 10^{-5} M and irradiation at 0, 1, 2, 4, 8, 12, 18, 24, 48 and 72 h of recovery in drug-free medium. Values (absorbance reported as percentage respect to the untreated cells, considered as 100%) are the average ± SD of three independent experiments. *values RBAc-PDT are significantly different ($p < 0.05$) with respect to the control value.

at each time of recovery post irradiation as indirectly measured by the MTT assay (**Fig. 1**). The lowest percentage of viable cells was measured after 48 h of recovery. RBAc-PDT significantly lowered lysosome enzyme activities. In fact, the incorporation of neutral red inside lysosomes was drastically reduced (**Fig. 2A**).

$DiOC_6(3)$ is a positively charged fluorescent molecule, able to permeate plasma membrane and localize in ER. In untreated cells, $DiOC_6(3)$ is observed in the entire cytoplasm, suggesting a random distribution of the ER inside the cell. At 24 h post irradiation, the fluorescence distribution indicates an initial fusion of ER vesicles, that progressively move towards the perinuclear region. At 48 and 72 h post irradiation, ER vesicles occupy a drastically reduced cytoplasmic area (**Fig. 2B**).

The ER stress induced by RBAc-PDT is confirmed by western blot analysis of whole cell lysates using an antibody specifically recognizing the cleaved caspase-12 (p40), that is significantly increased from 18 h after PDT until the end of recovery (**Fig. 3**).

A rapid release of Ca^{2+} ions from intracellular stores (likely mitochondria and ER) into the cytosol was spectrofluorimetrically measured with Fura-2 as soon as 1 h post irradiation (**Fig. 4**). The highest cytosolic $[Ca^{2+}]_i$ was measured at 12 h of post-PDT, 2.5 times the control.

RBAc-PDT mediated autophagy. The initial step of the autophagy is flat membrane cistern wrapping around a portion of cytosol and/or organelles forming a closed double-membrane bound vacuole containing cytosol and/or organelles, called *autophagosome* (devoid of any lysosomal proteins). Autophagosomes undergo a stepwise maturation process including fusion events with endosomal and/or lysosomal vesicles. In the autophagosomes fused with lysosomes, their content is degraded by lysosomal hydrolases. To study autophagy we used LC3B immunoblotting. Endogenous LC3B is the biochemical hallmark most commonly used for autophagy assay. Endogenous LC3B is detected as two bands following SDS-PAGE and immunoblotting: one represents LC3B-I (18 kDa), which is cytosolic, and the other LC3B-II (16 kDa), which is conjugated with phosphatidylethanolamine (PE), is present on isolated membranes and autophagosomes. During the recovery times after RBAc-PDT, LC3B-I protein constantly decreased in the cytosol (**Fig. 5A**). Its most significant decrements have been measured at 8, 48 and 72 h of recovery. Conversely, the LC3B-II protein dramatically increased on the membrane of autophagosomes at the 8 h post PDT and, due to the lysosomal digestion, progressively decreased (**Fig. 5A**). High levels of LC3B-II on membranes of autophagosomes were observed from 8 h post PDT to the end of experimental time in the presence of Bafilomycin A, a specific inhibitor of autophagosome-lysosome fusion (**Fig. 5B**).

Autophagy has been further analyzed by checking the presence of autophagosomes at 8 h of recovery post-PDT with TEM. Micrographs of **Figure 6A** show two examples of autophagosomes: one with the typical lamellae formation and the other with indigested material. HeLa cells bearing autophagosomes did not show chromatin condensation.

The induction of autophagy of RBAc-PDT treated HeLa cells, was further evaluated by using monodansylcadaverine added to cell culture medium, a selective marker for acidic vesicular organelles, such as autophagic vacuoles. Autophagosomes were analyzed by using fluorescence microscopy (**Fig. 6B**). Control HeLa cells showed a very scarce positivity for MDC (3% of positive cells), while the RBAc-PDT treated cells bore numerous MDC positive cytoplasmic vacuoles. At 8 h of recovery post PDT, 25% of HeLa cells were autophagic, while only 10% of autophagic HeLa cells was observed at 12 h post-PDT.

Inhibition of RBAc-PDT induced cell deaths. Inhibition of RBAc-PDT induced cell deaths was performed with pan-specific protease inhibitor, z-VAD and Necrostatin 1 (Nec-1) (**Fig. 7**). Neither z-VAD or Nec-1 completely prevented RBAc-PDT-induced cell death; indeed, 25 and 20% of cell deaths were measured respectively at 8 and 12 h post PDT, representing a reduction of deaths of about 40% (**Fig. 7A**). The entire 25% of dead cells measured in presence of inhibitors at 8 h post PDT, were MDC labeling positive HeLa cells, thus confirming the induction of autophagy. At 12 h post PDT, one half of the 20% of HeLa cells, dead in presence of z-VAD and Nec-1, was MDC positive (i.e., autophagic cells) (**Fig. 7C**), while the other half was positive only to Annexin V labeling (i.e., apoptotic cells) (**Fig. 7A**).

Discussion

In the current study we have demonstrated the induction of autophagy after RBAc-PDT in HeLa cells using different criteria.

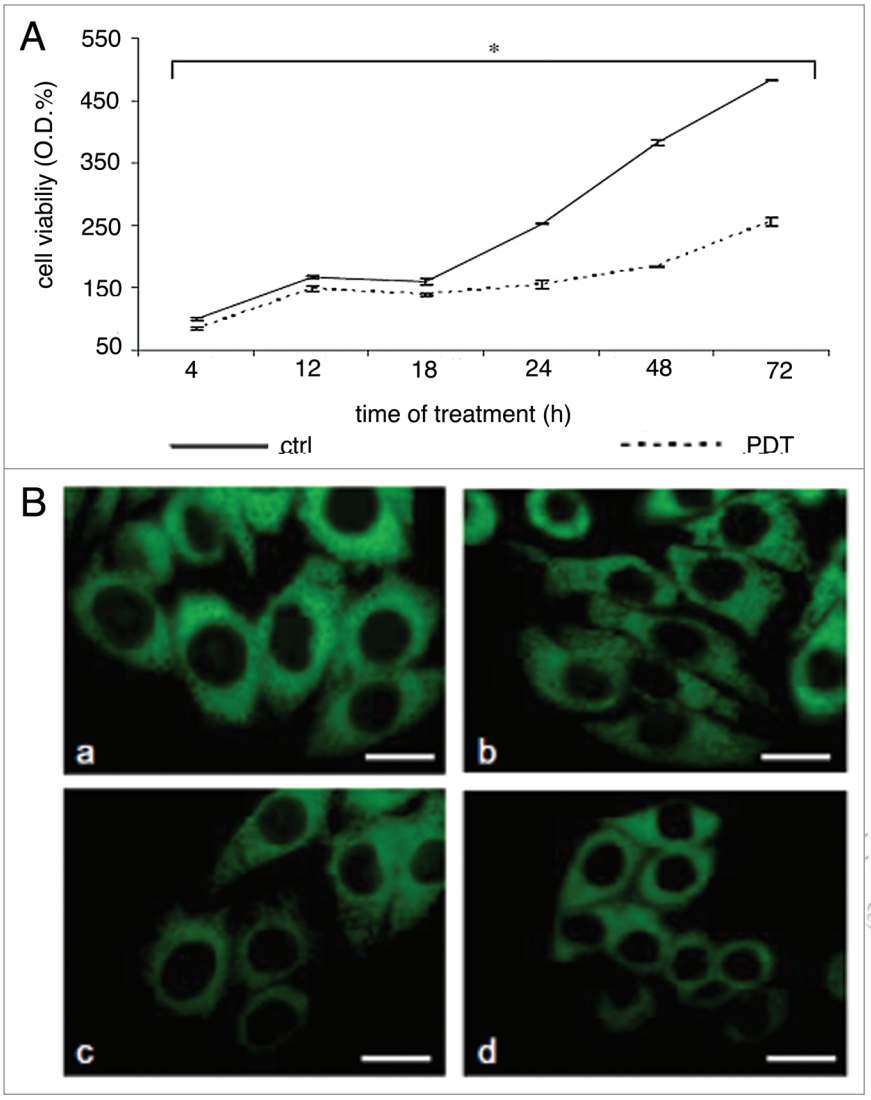

Figure 2. (A) NR assay performed in HeLa cells after treatment with RBAc 10^{-5} M and irradiation at 4, 12, 18, 24, 48 and 72 h of recovery in drug-free medium. Values (absorbance reported as percentage) are the mean of three independent experiments. *values RBAc-PDT are significantly different ($p < 0.05$) with respect to the corresponding control value. (B) $DiOC_6(3)$ (0.5 μg/ml) labeled control HeLa cells (a) and PDT-treated cells at 24 (b), 48 (c) and 72 h (d) of recovery in drug free medium; bars = 10 μm.

Although the studies that document the PDT-induced autophagy are increasing, they are still few and none of them used RBAc as photosensitizer.[9-13] Autophagy, originally described as a cell survival response, has also been implicated as a death pathway in numerous studies.[28-33] In the case of RBAc-PDT, autophagy plays a crucial role as suggested by the inhibition experiments with z-VAD and Nec-1. However, the basis for autophagy in RBAc-PDT has not been yet defined as in the case of CPO-PDT where autophagy derives by the photodamage to Bcl2.[18,34] It has been reported that the downregulation of Bcl2 expression induces/facilitates the onset of autophagy.[35,36] It could be hypothesized that the specific ROS-damaged subcellular site or organelle and the cargo of the autophagic vacuole are factors which could potentially influence the outcome of the autophagic process in RBAc-PDT-treated cells. Indeed, upon RBAc administration, the photoactive molecules of RB accumulate in perinuclear region and than diffuse dynamically throughout the cytoplasm.[20,37-40] Endosomes, Golgi apparatus and the ER are the precocious intracellular sites of accumulation of RB.[37,40,41] The photodamage to ER exerted by the RBAc-PDT, as demonstrated by the drastic reduced incorporation of $DiOC_6$ and by the increased level of cleaved caspase-12, promotes autophagy. However, the molecular mechanism leading to the removal of the damaged ER through the formation of the autophagosomes and their following fusion with the lysosomes for degradation during PDT, is not yet fully elucidated.[9] Recent studies have established that there are instances where the ER is preferentially targeted for autophagic degradation to support survival in yeast,[42,43] and autophagy is initiated following ER stress in mammalian cells.[44-47] Alternatively, due to the high reactivity of photogenerated ROS it is possible that autophagy is initiated in an attempt to remove organelles damaged by oxidation or to degrade large aggregates of cross-linked proteins, produced by photochemical reactions, which are not removed by the ubiquitin-proteasome system.[48]

Our criteria were: (1) the presence of multiple large vacuoles labeled with MDC; (2) conversion of LC3B-I to LC3B-II; (3) the presence of autophagosomes and absence of nuclear condensation by electron microscopy; (4) lysosomes; (5) the empty of Ca^{2+} from the ER; (6) the presence of cell death after caspase-dependent apoptosis and necrosis inhibition. All together our data confirm the induction of autophagy by the RBAc-PDT; in particular, those reported in **Figure** 7 indicated that autophagy is concomitantly induced along with apoptosis. Indeed, in previous works we reported that RBAc-PDT induced 35–40% of apoptosis in HeLa cells, mitochondria lost their membrane potential and released cytochrome-*c*.[26,27] The bulk of autophagic cells occurred quicker than apoptotic cells (8 vs. 12 h) and disappeared faster as well.

It is known that RBAc-PDT damages mitochondria as demonstrated by mitochondrial potential loss allowing the release of cytochrome *c*.[26,27] Examples of specific degradation pathways for damaged mitochondria, a process called mitophagy that often precedes apoptosis and requires caspase inhibition to be appreciated,[49] have been reported for hepatocytes and yeast.[50,51] It is thus likely that autophagy in RBAc-PDT HeLa cells occurs within the first 8 h post-PDT to eliminate damaged mitochondria, while apoptosis is maintained at high level by different caspase-dependent and -independent pathways. The

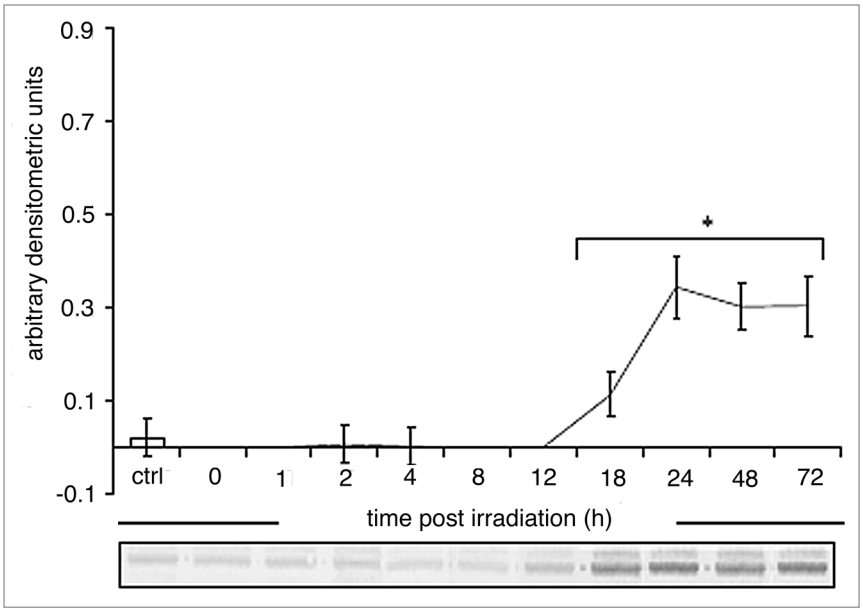

Figure 3. Kinetic of caspase-12 cleavage in HeLa cells. HeLa cells were subjected to RBAc-PDT (10^{-5} M RBAc, 1 h, 1.6 J/cm^2, 90 sec) and SDS-PAGE was performed on the cytosolic fraction obtained after irradiation at the indicated time intervals (30 μg protein/lane) and electroblotted to nitrocellulose membrane. Western blot was developed with specific antibody against cleaved caspase-12. Pattern of actin expression is used as a control. The antibody used detects cleaved product of caspase 12 (40 kDa). The amount of cleaved product of caspase 12 is reported as optical density (arbitrary densitometric units) measured by densitometer analysis. The data are the average ± SD of three independent experiments. *values RBAc-PDT are significantly different ($p < 0.05$) with respect to control value.

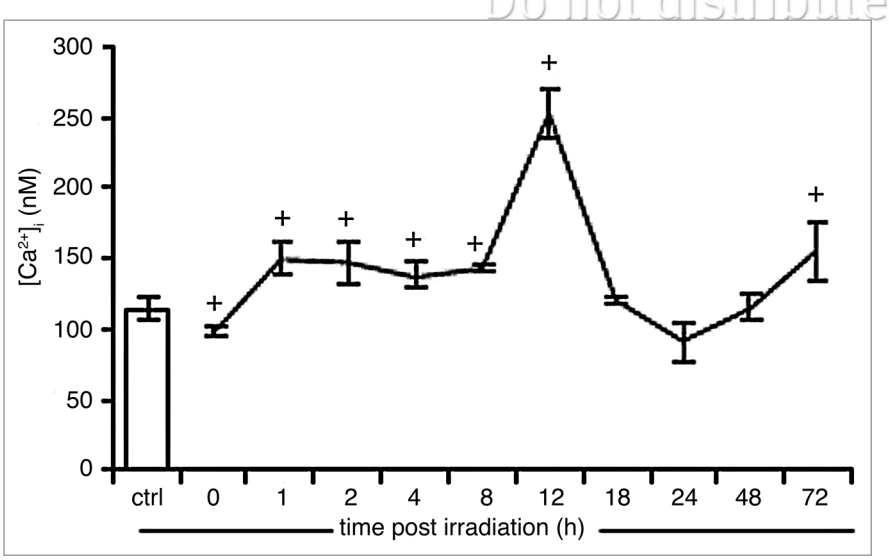

Figure 4. Evaluation of the concentration of $[Ca^{2+}]_i$ by Fura-2 in HeLa cells after treatment with RBAc 10^{-5} M and irradiation, followed by 0, 1, 2, 4, 8, 12, 18, 24, 48 and 72 h of recovery in drug-free medium. The data are the average ± SD of three independent experiments. *values RBAc-PDT are significantly different ($p < 0.05$) with respect to control value.

latter pathway seems to be particularly active at the longer time of recovery, contributing for a 10% of dead cells. It could be hypothesized that, since necrosis does not contribute to the killing of cells in our in vitro system, the induction of inflammation that accompanies necrosis is prevented also in vivo. In addition, the fast removal of apoptotic cells that is a peculiarity of the apoptotic process, represents an additional mechanism to prevent inflammation.[52]

More studies are required to define the still uncertain functional contribution of this catabolic process in cell death and whether autophagy directly contributes to death or is a failed effort to preserve cell viability. In addition, the molecular mediators which may turn autophagy into a cell death pathway and the cross-talk between autophagy and the apoptotic machinery in PDT-exposed cells need to be better identified. As in apoptosis, there is a flipping of phosphatidylserine to the cell surface during autophagy.[35] Externalization of phospshatidylserine enables the dying cells to be recognized and phagocytized most likely avoiding an inflammatory response. Last, it is interesting to note that autophagy can result in class II presentation of antigens derived from cytosolic proteins,[36] may therefore provide an explanation for the finding that treatment of tumor cells with low-dose PDT can yield anti-tumor vaccines.[53]

Materials and Methods

Chemicals. RBAc was obtained as a colorless powder by acylation of RB (Fluka Chemie, Buchs, Switzerland) according to a procedure already described.[20] A stock solution (10^{-2} M) was obtained by diluting RBAc in dimethyl sulfoxide: final concentration (10^{-5} M) was obtained directly in the culture medium at the time of incubation. All other chemicals used were of the commercially available highest purity. Unless otherwise stated, all the chemicals are purchased from Sigma Chem. Co. (St. Louis, Mo, USA).

Cell culture. Human epithelioid cervix carcinoma cells (HeLa) were cultured in Eagle's minimum essential medium (EMEM) (Cambrex, Verviers, Belgium) supplemented with 10% fetal calf serum (FCS), 2 mM L-glutamine (Cambrex, Verviers, Belgium), 100 IU/ml penicillin and streptomycin solution and 10000 U/ml nystatin (antimicotic solution) (Cambrex, Verviers, Belgium), in a 5% CO_2 humidified atmosphere at 37°C. Cells were maintained in 75 cm^2 flasks (concentration ranged between 2 x 10^5 and 1 x 10^6 cells/ml) by passage every 3 to 4 days.

PDT treatment. Cells were incubated for 60 minutes at 37°C with RBAc (10^{-5} M) in EMEM medium supplemented with

10% FCS. After incubation, the culture medium was replaced with phosphate buffer saline (0.2 M PBS, pH 7.4), previously allowed to equilibrate with 5% CO_2 humidified atmosphere, without phenol red, to avoid undesired photosensitizing effects. Cells were then exposed for 90 seconds to innovative green light emitting diode, LED DPL 305, (QTL Inc., Atlanta, USA) emitting at 530 ± 15 nm, in order to obtain 1.6 J/cm^2 as total light dose. After irradiation cells were rinsed twice with PBS 0.2 M pH 7.4, transferred to drug-free complete medium and allowed to recover for different times (from 0 to 72 h).

Cell viability assays. *MTT.* 3-(4,5-dimethylthiazol-2-yl)-2,5-diphenyltetrasolium bromide (MTT) assay (MTT 98% Sigma-Aldrich) that is a cytotoxicity method, was performed according to the modified MTT method described by Sladowski et al.[21] Briefly, at fixed recovery times following the RBAc incubation and irradiation, cells were incubated with 1 mg/ml MTT in culture medium for 2 hours. After extensive washing in PBS, living cells were determined by MTT dye reduction. The amount of MTT-formazan produced is directly associated with cell viability and it can be determined spectrophotometrically (DU 640 B, Beckman Coulter, USA) at 570 nm after solubilization of crystal in 1 ml of DMSO.

NR assay. Lysosomal activity was evaluated by the neutral red (NR) assay. The culture medium was replaced with 1.0 ml/well of neutral red solution (0.01% in culture medium) and the cells were incubated for 2 hours at 37°C. After rinsing with PBS, 1 ml/well of stain extraction solution (1% glacial acetic acid, 50% ethanol, 49% distilled water) was added. The plates were shaken for 10 minutes and the absorbance was read at 540 nm with a spectrophotometer (DU640B, Beckman Coulter, USA). The NR assay, together with the MTT and Kenacid Blue assays, has been extensively used in other studies of cell viability in cytotoxicity assessments. The NR assay can also be used as a vital stain.

Endoplasmic reticulum damage evaluation. *$DiOC_6(3)$ staining.* At different recovery times after PDT-treatment, living cells were washed three times with PBS (0.2 M pH 7.4) and stained with 3,3'-dihexyloxacarbocyanine iodide ($DiOC_6(3)$; 0.5 μg/ml in complete culture medium in a 5% CO_2 humidified atmosphere at 37°C for 10 min). $DiOC_6(3)$ is a marker of the endoplasmic reticulum (ER).[22]

Immunoblot analysis of caspase-12 activation. HeLa cells were collected by Trypsin/EDTA 0.25%, washed in ice-cold PBS, suspended in lysis buffer (Tris-HCl 50 mM pH 7.4, DTT 10 mM and PMFS 1 mM) and further centrifuged at 10,000 g for 10 min. In order to separate cytosol and membrane proteins, samples were centrifuged at 36,000 g for 1 h. The pellet, containing membrane proteins, was suspended in Tris-HCl 1 mM-DTT 50 mM-PMFS 1 mM. Proteins were delipidated by different passages in methanol/chloroform. The supernatant, containing cytosol proteins, was precipitated in acetone. Proteins were suspended in sample buffer (Tris-HCl 0.0625 M pH 6.8, Glycerol 10%, SDS 2%, DTT 50 mM and PMFS 1 mM) and solubilized in a boiling water bath for 5–6 min. Protein concentration was determined by Bio-Rad protein assay.[23]

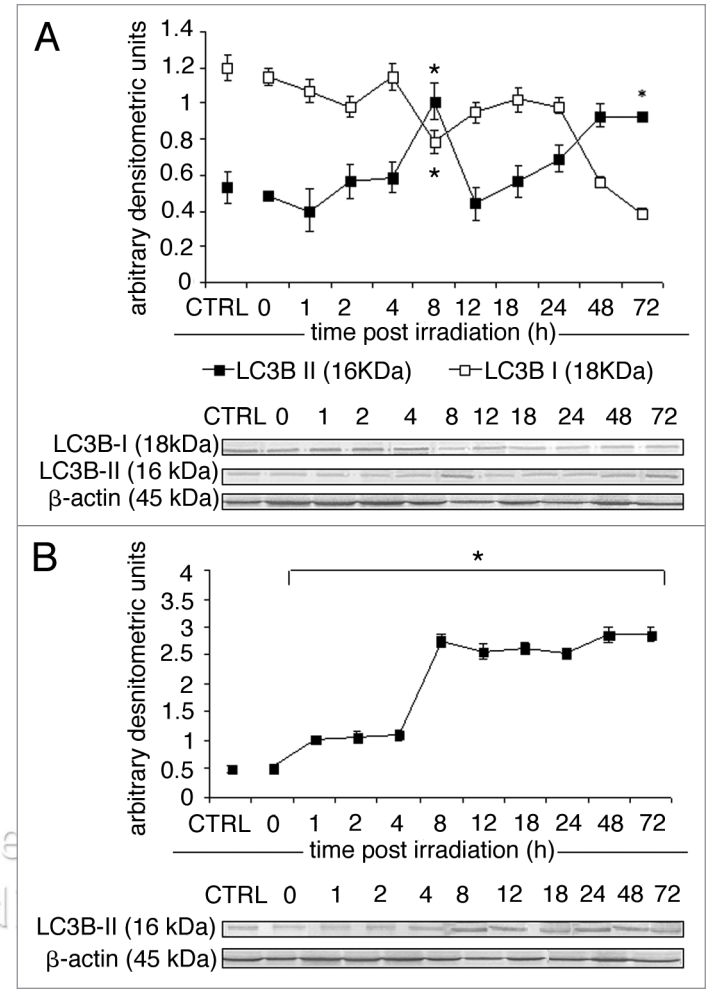

Figure 5. (A) Kinetic of LC3B cleavage. The HeLa cells were subjected to RBAc-PDT (10^{-5} M RBAc, 1 h, 1.6 J/cm^2, 90 sec) and SDS-PAGE was performed on the cytosolic and membrane fraction obtained after irradiation at the indicated time intervals (30 μg protein/lane) and electroblotted to nitrocellulose membrane. Western blot was developed with specific antibody against LC3B. Pattern of actin expression is shown as a control. The antibody used detects 18 kDa protein LC3B (LC3B-I). In autophagic cells the antibody also detects 16 kDa protein, corresponding to the cleaved form of LC3B (LC3B-II). The amount of LC3B-I and LC3B-II proteins were reported as optical density (arbitrary densitometric units) measured by densitometer analysis. The data are the average ± SD of three independent experiments. *values RBAc-PDT are significantly different ($p < 0.05$) with respect to control value. (B) Kinetic of LC3B cleavage in presence of Bafilomycin A. The HeLa cells were subjected to RBAc-PDT (10^{-5} M RBAc, 1 h, 1.6 J/cm^2, 90 sec) in presence of Bafilomycin A (100 nM) and SDS-PAGE was performed on the membrane fraction obtained after irradiation at the indicated time intervals (30 μg protein/lane) and electroblotted to nitrocellulose membrane. Western blot was developed with specific antibody against LC3B-II (18 kDa). Pattern of actin expression is shown as a control. The amount of LC3B-II protein was reported as optical density (arbitrary densitometric units) measured by densitometer analysis. The data are the average ± SD of three independent experiments. *values RBAc-PDT are significantly different ($p < 0.05$) with respect to control value.

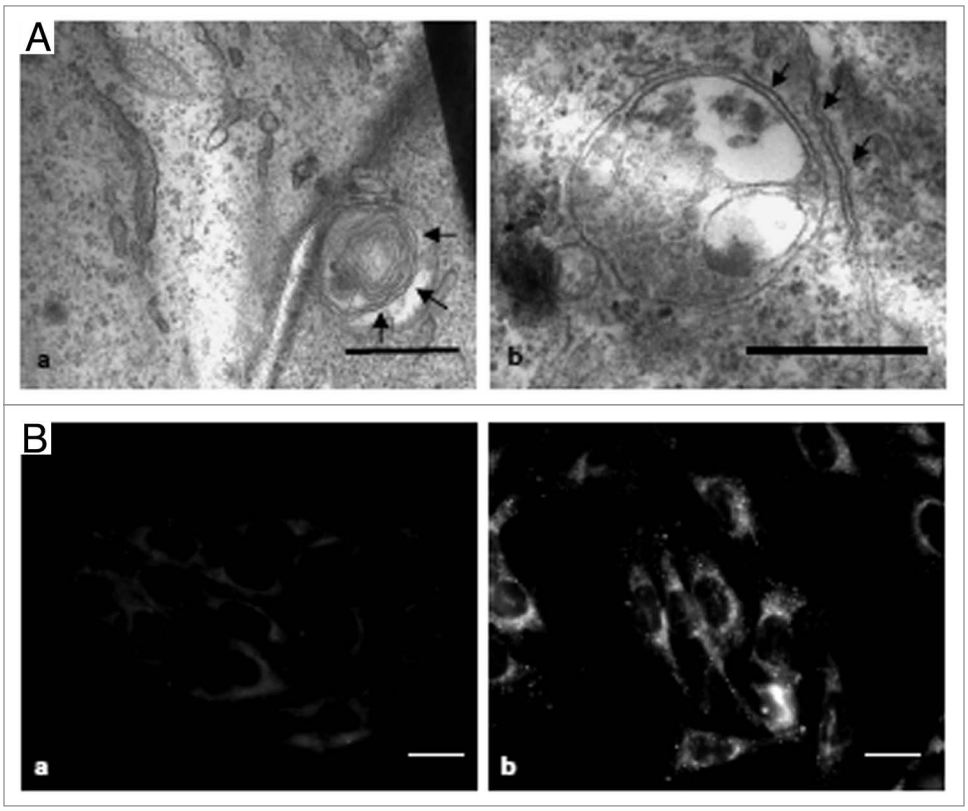

Figure 6. (A) Electron microscopy (TEM) micrographs of HeLa cells at 8 h of recovery post PDT treatment (a and b) showing the presence of autophagosomes. Arrows show examples of autophagosomes with the typical lamellae formation. In (b) is shown a representative autophagosoma with degenerating material. Bars = 0.5 μm. (B) Fluorescence microscopy micrographs of Monodansylcadaverine (MDC) (0.05 mM) labeled control HeLa cells (a) and PDT-treated cells at 8 h of recovery (b); bars = 10 μm.

Proteins (30 μg) were separated by 13% SDS-PAGE under reducing conditions, followed by western Blotting. Membranes were blocked for 1 h in TBS 25 mM pH 8.3/3% BSA.

The following primary antibodies were incubated with the appropriate membranes: anti-actin diluted 1:2,000 and anti-caspase-12 diluted 1:200 (MBL, Woburn, MA, USA). Appropriate IgG Biotin-conjugated secondary antibody, diluted 1:2,000, was incubated with the membranes for 2 h. The membranes were incubated with ExtrAvidin peroxidase diluted 1:1,500 at 4°C for 1 h. After each incubation with antibody and prior to the addition of DAB solution for 20 min in the dark, membranes were washed three times in TBS 25 mM pH 8.3. The densitometer analysis was performed with a GS-700 Imaging Densitometer (Bio-Rad).

Autophagy evaluation. *MDC staining.* HeLa cells were stained with 0.05 mM monodansylcadaverine (MDC) (Fluka Chemie, Buchs, Switzerland) in PBS after PDT treatment at room temperature (RT) for 10 min.[24] Cells were washed two times with phosphate buffered saline (PBS) and immediately observed using the fluorescence microscope Eclipse 80i (Nikon, Tokyo, Japan). Counts were performed on at least 20 randomly chosen microscopic fields (x40) and at least 300 nuclei were analyzed.

TEM. The presence of autophagosone vacuoles in HeLa cells was investigated with a transmission electron microscope (TEM). Cells were fixed with 2.5% glutaraldehyde in cacodylate buffer, pH 7.4, for 1 h at ice temperature and postfixed with 1% OsO_4 in the same buffer. Samples were dehydrated, embedded in Spurr resin and examined under a Zeiss 910 transmission electron microscope operating at 80 kV.

Immunoblot analysis of LC3B protein. The PDT treatment was performed also in presence of Bafilomycin A, a specific inhibitor of autophagosome-lysosome fusion. For experiments of inhibition, HeLa cells were incubated for 60 minutes at 37°C with RBAc 10^{-5} M and Bafilomycin A 100 nM in EMEM medium supplemented with 10% FCS. After PDT treatment, cells were transferred to RBAc-free EMEM medium (10% FCS) supplemented with Bafilomycin A 100 nM and allowed to recover for different times (from 0 to 72 h). A stock solution (1.5 mM) of Bafilomycin A was obtained by dilution in dimethyl sulfoxide: final concentration (100 nM) was obtained directly in the culture medium at the time of incubation. At the end of experiment, HeLa cells were subjected to western blot analysis, by using a primary antibody for LC3B protein diluted 1:500 (MBL, Woburn, MA), as above reported.

Measurements of Ca^{2+} levels. HeLa cells, washed twice with loading buffer (107 mM NaCl, 5 mM KCl, 7 mM $NaHCO_3$, 3 mM $CaCl_2$, 1 mM $MgSO_4 \bullet 6H_2O$, 20 mM Hepes, 10 mM glucose, 0.1% BSA) and resuspended at a concentration of 1 x 10^6/ml, were incubated with 4 μM Fura-2 acetoxymethylesther (Fura2-AM) for 45 min at 37°C in a 5% CO_2 humidified atmosphere at 37°C.

After the dye loading, cells were washed twice with the same loading buffer and then re-suspended in fresh loading buffer at the final concentration of 7 x 10^6 cells/ml. Cells were stored at room temperature until use and pre-warmed at 37°C for 20 min before measurements. 20 μl of this cell suspension was added to a 2 ml of loading buffer in a fluorescence cuvette kept at 21°C and stirred through-out the experiment. The fluorescence intensity of Fura-2 was measured with a Jasco FP-750 spectrofluorometer, equipped with an electronic stirring system and a thermostabilized (37°C) cuvette holder and monitored by a personal computer running the Jasco Spectra Manager software for Windows 95 (Jasco Europe S.r.l., Lecco, Italy). The excitation wavelengths were 340 nm and 380 nm and the emission wavelength is 510 nm; the slit widths were set to 10 nm. The maximal fluorescence (F_{max}) value was determined at the end of each experiment by

adding 20 μl of 20% SDS; the minimal fluorescence (F_{min}) value was determined by adding 20 μl of 0.5 M of EGTA solution, pH 9.0. The cytoplasmic Ca^{2+} concentration at time *t* was calculated by using the software of the fluorimeter with the calculated dissociation constant (K_d = 224 nm) for the Fura-2-Ca^{2+} complex, according to Grynkiewicz equation:[25]

$$[Ca^{2+}, nM]_t = K_d (F_t - F_{min}) F_{min,380} / (F_{max} - F_t) F_{max,380}$$

where *F* denotes the time course of the florescence at 510 nm after dual excitation at 340/380 nm and F_{380} is the fluorescence at 510 nm after excitation at 380 nm.

Cell death inhibition. In cell death inhibition experiments, apoptosis was inhibited by using pan-caspase inhibitor z-VAD (20 μM, R&D System, Minneapolis, MN, USA) and necrosis by using Necrostatin-1 (300 μM, Santa Cruz Biotechology, Inc., Santa Cruz, California, USA). The cell death inhibitors were added alone and in presence or absence of both inhibitors 30 minutes before photodynamic treatment, during RBAc treatment (1 h incubation) and after irradiation during recovery times (8, 12 and 24 h) in a 5% CO_2 humidified atmosphere at 37°C. Dead cells were evaluated by using the AnnexinV/PI and MDC staining.

Annexin V/PI staining. Dead cells were detected by using AnnexinV-FITC Apoptosis Detection Kit (Sigma St. Louis, MO, USA). Cells were rinsed twice with PBS 0.2 M pH 7.4 and incubated for 10 min in complete culture medium containing 0.5 μg/ml FITC-conjugated Annexin V and 2 μg/ml Propidium Iodide (PI). Dead cells were recognized with a fluorescence microscope Eclipse 80i (Nikon, Tokyo, Japan) for their positivity to Annexin V, that binds the phosphatidylserine residues translocated to the outer leaflet of the plasma membrane. Early apoptotic cells were only stained by Annexin V-FITC, necrotic cells were simultaneously stained by PI and Annexin V-FITC and living cells were not stained. Counts were performed on at least 20 randomly chosen microscopic fields (40x) and at least 300 cells were analyzed.

Statistical analysis. The two-tailed Student's t-test was used to analyze differences between controls and treated samples. Data are presented as mean value ± SD and all tests were performed at the 0.05 significance level.

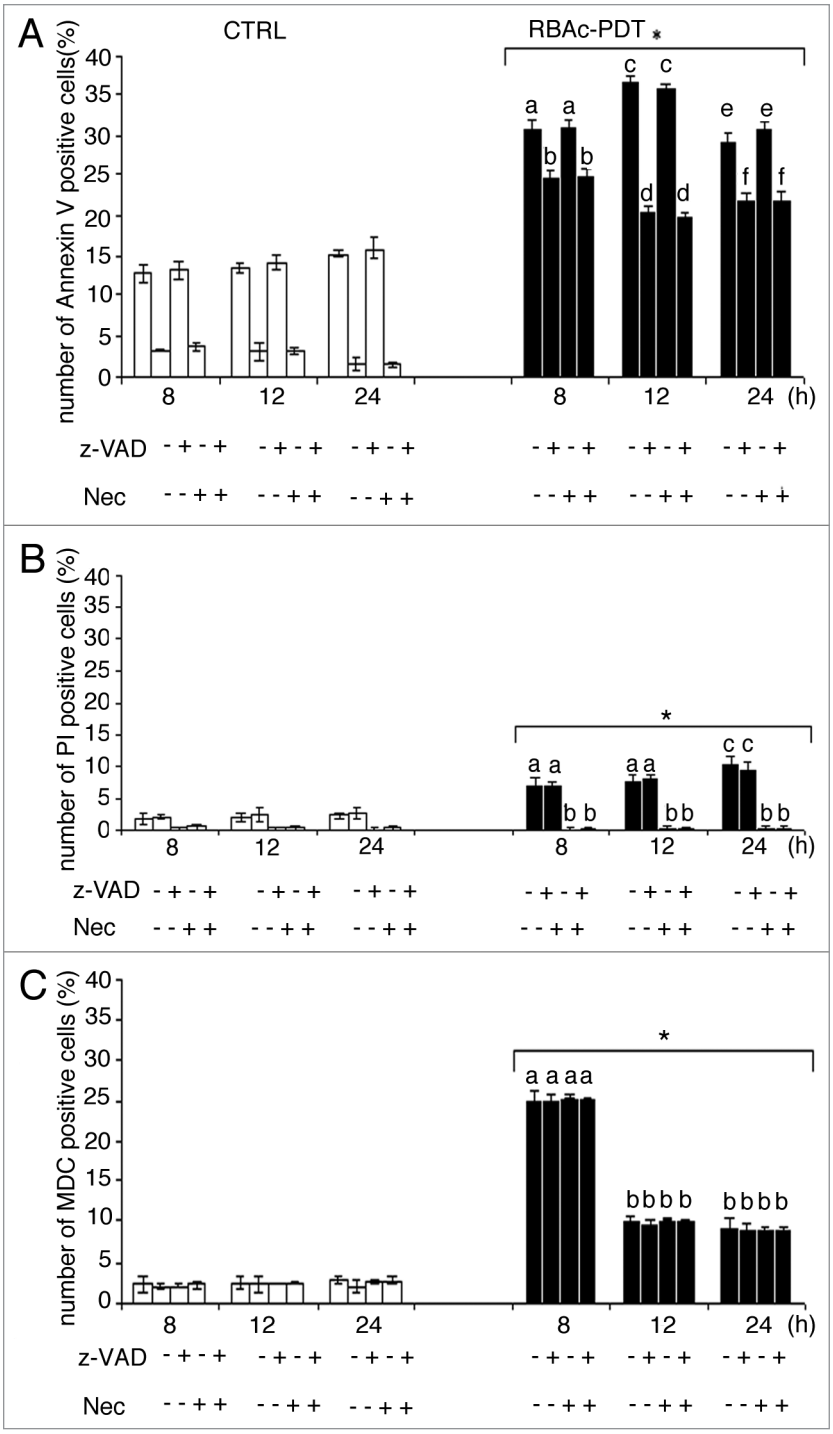

Figure 7. Time course of apoptosis of HeLa cells following RBAc-PDT. Cells were subjected to RBAc-PDT (10^{-5} M RBAc, 1 h, 1.6 J/cm^2, 90 sec) in the presence of pan-caspases inhibitor (z-VAD) and necrosis inhibitor Necrostatin-1 (Nec-1). (A) Percentage number of Annexin V positive control and RBAc-PDT treated HeLa cells (i.e., apoptotic and autophagic dead cells). (B) Percentage number of Propidium Iodide (PI) positive control and RBAc-PDT treated HeLa cells (i.e., necrotic dead cells). (C) Percentage number of Monodansylcadaverine (MDC) positive control and RBAc-PDT treated HeLa cells (i.e., autophagic dead cells). The fractions of dead cells were determined at 8, 12 and 24 h after irradition. At least 500 cells per samples were counted. Values are the average ± SD of three independent experiments. Results that are significantly different ($p < 0.05$) between the samples are indicated by different characters above the columns. *values RBAc-PDT are significantly different ($p < 0.05$) with respect to control values.

References

1. Ochsner M. Photophysical and photobiological processes in the photodynamic therapy of tumours. J Photochem Photobiol B 1997; 39:1-18.
2. Juarranz A, Jaén P, Sanz-Rodríguez F, Cuevas J, González S. Photodynamic therapy of cancer. Basic principles and applications. Clin Transl Oncol 2008; 10:148-54.
3. Dougherty TJ, Gomer CJ, Henderson BW, Jori G, Kessel D, Korbelik M, et al. Photodynamic therapy. J Natl Cancer Inst 1998; 90:889-905.
4. Milanesi C, Zhou C, Biolo R, Jori G. Zn(II)-phthalocyanine as a photodynamic agent for tumours. II. Studies on the mechanism of photosensitised tumour necrosis. Br J Cancer 1990; 61:846-50.
5. Agarwal ML, Clay ME, Harvey EJ, Evans HH, Antunez AR, Oleinick NL. Photodynamic therapy induces rapid cell death by apoptosis in L5178Y mouse lymphoma cells. Cancer Res 1991; 51:5993-6.
6. Chiu SM, Xue LY, Usuda J, Azizuddin K, Oleinick NL. Bax is essential for mitochondrion-mediated apoptosis but not for cell death caused by photodynamic therapy. Br J Cancer 2003; 89:1590-7.
7. Buytaert E, Callewaert G, Hendrickx N, Scorrano L, Hartmann D, Missiaen L, et al. Role of the endoplasmic reticulum depletion and multidomain proapoptotic BAX and BAK proteins in shaping cell death after hypericin-mediated photodynamic therapy. FASEB J 2006; 20:756-8.
8. Whitacre CM, Satoh TH, Xue L, Gordon NH, Oleinick NL. Photodynamic therapy of human breast cancer xenografts lacking caspase-3. Cancer Lett 2002; 179:43-9.
9. Reiners JJ Jr, Agostinis P, Berg K, Oleinick NL, Kessel D. Assessing autophagy in the context of photodynamic therapy. Autophagy 2010; 6:7-18.
10. Kessel D. Protection of Bcl-2 by salubrinal. Biochem Biophys Res Commun 2006; 346:1320-23.
11. Xue LY, Chiu SM, Azizuddin K, Joseph S, Oleinick NL. The death of human cancer cells following photodynamic therapy: apoptosis competence is necessary for Bcl-2 protection but not for induction of autophagy. Photochem Photobiol 2007; 83:1016-23.
12. Davids LM, Kleemann B, Cooper S, Kidson SH. Melanomas display increased cytoprotection to hypericin-mediated cytotoxicity through the induction of autophagy. Cell Biol Int 2009; 33:1065-72.
13. Sasnauskiene A, Kadziauskas J, Vezelyte N, Jonusiene V, Kirveliene V. Apoptosis, autophagy and cell cycle arrest following photodamage to mitochondrial interior. Apoptosis 2009; 14:276-86.
14. Buytaert E, Dewaelea M, Agostinis P. Molecular effectors of multiple cell death pathways initiated by photodynamic therapy. Biochim Biophys Acta 2007; 1776:86-107.
15. Ferraro E, Cecconi F. Autophagic and apoptotic response to stress signals in mammalian cells. Arch Biochem Biophys 2007; 462:210-9.
16. Yue Z, Jin S, Yang C, Levine AJ, Heintz N. Beclin 1, an autophagy gene essential for early embryonic development, is a haploinsufficient tumor suppressor. Proc Natl Acad Sci USA 2003; 100:15077-82.
17. Kroemer G, Galluzzi L, Vandenabeele P, Abrams J, Alnemri ES, Baehrecke EH, et al. Classification of cell death: recommendations of the Nomenclature Committee on Cell Death 2009. Cell Death Differ 2009; 16:3-11.
18. Kessel D, Vicente MG, Reiners JJ. Initiation of apoptosis and autophagy by photodynamic therapy. Lasers Surg Med 2006; 38:482-8.
19. Vantieghem A, Xu Y, Assefa Z, Piette J, Vandenheede JR, Merlevede W, et al. Phosphorylation of Bcl-2 in G_2/M phase-arrested cells following photodynamic therapy with hypericin involves a CDK1-mediated signal and delays the onset of apoptosis. J Biol Chem 2002; 277:37718-31.
20. Bottiroli G, Croce AC, Balzarini P, Locatelli D, Baglioni P, Lo Nostro P, et al. Enzyme-assisted cell photosensitization: a proposal for an efficient approach to tumor therapy and diagnosis. The rose Bengal fluorogenic substrate. Photochem Photobiol 1997; 66:374-83.
21. Sladowski D, Steer SJ, Clothier RH, Balls M. An improved MTT assay. J Imm Meth 1993; 157:203-7.
22. Sabnis RW, Deligeorgiev TG, Jachak MN, Dalvi TS. $DiOC_6$: a useful dye for staining the endoplasmic reticulum. Biotech Histochem 1997; 72:253-8.
23. Bradford MM. A rapid and sensitive method for the quantification of microgram quantities of protein utilizing the principle of protein-dye binding. Anal Biochem 1976; 72:248-54.
24. Biederbick A, Kern HF, Elsässer HP. Monodansylcadaverine (MDC) is a specific in vivo marker for autophagic vacuoles. Eur J Cell Biol 1995; 66:3-14.
25. Grynkiewicz G, Poenie M, Tsien RJ. A new generation of Ca^{2+} indicators with greatly improved fluorescence properties. Biol Chem 1995; 260:3440-50.
26. Panzarini E, Tenuzzo B, Palazzo F, Chionna A, Dini L. Apoptosis induction and mitochondria alteration in human HeLa tumor cells by photoproducts of Rose Bengal acetate. J Photochem Photobiol B 2006; 83:39-47.
27. Panzarini E, Tenuzzo B, Dini L. Photodynamic therapy-induced apoptosis of HeLa cells. Ann NY Acad Sci 2009; 1171:617-26.
28. Gozuacik D, Kimchi A. Autophagy as a cell death and tumor suppressor mechanism. Oncogene 2004; 23:2891-906.
29. Yu L, Alva A, Su H, Dutt P, Freundt E, Welsh S, et al. Regulation of an ATG7-beclin 1 program of autophagic cell death by caspase-8. Science 2004; 304:1500-2.
30. Edinger AL, Thompson CB. Death by design: apoptosis, necrosis and autophagy. Curr Opin Cell Biol 2004; 16:663-9.
31. Eskelinen EL. Maturation of autophagic vacuoles in Mammalian cells. Autophagy 2005; 1:1-10.
32. Tsujimoto Y, Shimizu S. Another way to die: autophagic programmed cell death. Cell Death Differ 2005; 12:1528-34.
33. Lockshin RA, Zakeri Z. Apoptosis, autophagy and more. Int J Biochem Cell Biol 2004; 36:2405-19.
34. Xue LY, Chiu SM, Fiebig A, Andrews DW, Oleinick NL. Photodamage to multiple Bcl-x_L isoforms by photodynamic therapy with the phthalocyanine photosensitizer Pc 4. Oncogene 2003; 22:9197-204.
35. Melino G, Knight RA, Nicotera P. How many ways to die? How many different models of cell death? Cell Death Diff 2005; 12:1457-62.
36. van der Bruggen P, van den Eynde BJ. Processing and presentation of tumor antigens and vaccination strategies. Curr Opin Immunol 2006; 18:98-104.
37. Bottiroli G, Croce AC, Biggiogera M, Lanza KS, Fiorani S, Locatelli D. Photosensitizer damage targets in Rose Bengal acetate treated cells. Lasers Surg Med Suppl 2001; 13:41-173.
38. Croce AC, Locatelli D, Monici M, Spano A, Pippia P, Bernabei P, et al. Application of Xuorogenic substrates to photodynamic therapy: rose bengal acetate. Lasers Surg Med Suppl 1997; 9:26-121.
39. Croce AC, Supino R, Lanza KS, Locatelli D, Baglioni P, Bottiroli G. Photosensitizer accumulation in spontaneous multidrug resistant cells: a comparative study with rhodamine 123, rose bengal and photofrin. Photochem Photobiol Sci 2002; 1:71-8.
40. Bottone MG, Soldani C, Fraschini A, Alpini C, Croce AC, Bottiroli G, et al. Enzyme-assisted photosensitization with rose Bengal acetate induces structural and functional alteration of mitochondria in HeLa cells. Histochem Cell Biol 2007; 127:263-71.
41. Soldani C, Bottone MG, Croce AC, Fraschini A, Bottiroli G, Pellicciari C. The Golgi apparatus is a primary site of intracellular damage after photosensitization with Rose Bengal acetate. Eur J Histochem 2004; 48:443-8.
42. Bernales S, McDonald KL, Walter P. Autophagy counterbalances endoplasmic reticulum expansion during the unfolded protein response. PLoS Biol 2006; 4:2312-24.
43. Yorimitsu T, Nair U, Yiang Z, Klionsky DJ. Endoplasmic reticulum stress triggers autophagy. J Biol Chem 2006; 281:30299-304.
44. Ogata M, Hino S, Saito A, Morikawa K, Kondo S, Kanemoto S, et al. Autophagy is activated for cell survival after endoplasmic reticulum stress. Mol Cell Biol 2006; 26:9220-31.
45. Kouroku Y, Fujita E, Tanida I, Ueno T, Isoai A, Kumagai H, et al. ER stress (PERK/eIF2alpha phosphorylation) mediates the polyglutamine-induced LC3 conversion, an essential step for autophagy formation. Cell Death Differ 2007; 14:230-9.
46. Criollo A, Maiuri MC, Tasdemir E, Vitale I, Fiebig AA, Andrews D, et al. Regulation of autophagy by the inositol trisphosphate receptor. Cell Death Differ 2007; 14:1029-39.
47. Hoyer-Hansen M, Bastholm L, Szyniarowski P, Campanella M, Szabadkai G, Farkas T, et al. Control of macroautophagy by calcium, calmodulin-dependent kinase kinase-beta and Bcl-2. Mol Cell 2007; 25:193-205.
48. Dewaele M, Martinet W, Rubio N, Verfaillie T, de Witte PA, Piette J, et al. Autophagy pathways activated in response to PDT contribute to cell resistance against ROS damage. J Cell Mol Med 2010; In press.
49. Kundu M, Thompson CB. Macroautophagy versus mitochondrial autophagy: a question of fate? Cell Death Differ 2005; 12:1484-9.
50. Elmore SP, Qian T, Grissom SF, Lemasters JJ. The mitochondrial permeability transition initiates autophagy in rat hepatocytes. FASEB J 2001; 15:2286-7.
51. Kissova I, Deffieu M, Manon S, Camougrand N. Uth1p is involved in the autophagic degradation of mitochondria. J Biol Chem 2004; 279:39068-74.
52. Maderna P, Godson C. Phagocytosis of apoptotic cells and the resolution of inflammation. Biochim Biophys Acta 2003; 1639:141-51.
53. Gollnick SO, Vaughan L, Henderson BW. Generation of effective antitumor vaccines using photodynamic therapy. Cancer Res 2002; 62:1604-8.